30p.

N 62 13753

NASA TN D-1355

NASA TN D-1355

USE FILE COPY

TECHNICAL NOTE

D-1355

EXPERIMENTAL INVESTIGATION OF THE EFFECT OF CONVECTIVE AND RADIATIVE HEAT LOADS ON THE PERFORMANCE OF SUBLIMING AND CHARRING ABLATORS

By Roger W. Peters and R. Gale Wilson

Langley Research Center
Langley Station, Hampton, Va.

NATIONAL AERONAUTICS AND SPACE ADMINISTRATION

WASHINGTON July 1962

K

NATIONAL AERONAUTICS AND SPACE ADMINISTRATION

TECHNICAL NOTE D-1355

EXPERIMENTAL INVESTIGATION OF THE EFFECT OF CONVECTIVE AND RADIATIVE HEAT LOADS ON THE PERFORMANCE OF SUBLIMING AND CHARRING ABLATORS

By Roger W. Peters and R. Gale Wilson

L
1
8
2
0

SUMMARY

A limited number of combined convective heating and radiative heating tests in a subsonic arc jet augmented by a cylindrical graphite-grid radiator have shown that the efficiency of a charring ablator, such as phenolic-nylon, increases with increasing heat load, regardless of whether the heat input is radiative or convective, because the higher surface temperatures promote increased reradiation. The efficiency of subliming ablators, though not appreciably influenced by the magnitude of the total heating rate, is significantly affected by the radiative heat input. The efficiency of the transparent sublimer, Teflon, is reduced almost to zero by the radiative input. The efficiency of the nearly opaque sublimer, Fluorogreen, is only slightly reduced by the radiative input.

INTRODUCTION

The heat-shielding characteristics of ablating materials for use on reentry vehicles have been investigated in a wide variety of arc-powered air jets and tunnels, rocket exhaust systems, and ceramic-heated jets (ref. 1). These facilities generally provide only a convective heat load or an ill-defined radiant heat load. However, reentry of a blunt-shaped body at velocities approaching escape velocity (36,000 feet per second) may result in radiative heat loads equal to or exceeding the convective heat loads. The question arises as to whether the ablating materials, which have been found to be satisfactory in a purely convective heating environment, will perform satisfactorily in a radiative or a combined radiative-convective heating environment. To answer this question, a study was made of the influence of convective, radiative, and combined convective-radiative heat loads on the performance of ablating materials. Two subliming ablators and one charring ablator were tested in a subsonic arc jet equipped with a cylindrical radiator to provide various combinations of convective and radiative heating. Some

preliminary data were presented in reference 2, and it is the purpose of this paper to present more complete results of this investigation.

SYMBOLS

A	area, sq ft
$F_{1,3}$	configuration factor for radiative heat transfer from area A_1 to area A_3
$F_{2,3}$	configuration factor for radiative heat transfer from area A_2 to area A_3
l	length, ft
q	heating rate to black body, Btu/ft^2-sec
r	radius of circular area, ft
S	distance between radiator and specimen, ft
T	absolute temperature, $^{\circ}$R
ϵ	emittance of radiator surface
σ	Stefan-Boltzmann constant, Btu/(ft^2)($^{\circ}$R)^4(sec)

Subscripts:

1	inside cylindrical surface area of radiator
2	cross-sectional (end) surface area of radiator
3	irradiated area of specimen
c	convective
i	inside radius of radiator
o	outside radius of radiator
r	radiative
T	total

TEST EQUIPMENT

2,500-Kilowatt Arc Jet

The convective heating tests were performed in a 2,500-kilowatt arc jet at the Langley Research Center. This facility, shown in figures 1 and 2, consists of a water-cooled copper chamber in which are located three pairs of concentric ring electrodes fabricated of copper tubing. Each pair of ring electrodes is water cooled and is energized by one phase of a three-phase alternating-current power supply. The arc drawn between each pair of concentric ring electrodes is rotated in the plane of the electrodes by a direct-current magnetic field induced by the coils surrounding the arc chamber. Compressed air, introduced at the bottom of the chamber through the electrode holders, is heated on passing through the arc region. The heated air exits through a water-cooled nozzle at the top of the arc chamber. For most of the tests reported herein, a 4-inch-diameter nozzle was used. One test utilized a 3-inch-diameter nozzle, and one test utilized a 6-inch-diameter nozzle. The conditions provided for the tests are enumerated in table I. For these conditions the enthalpy is approximately 3,000 Btu/lb based on the measured time-averaged maximum stream temperature.

L
1
8
2
0

Cylindrical Graphite-Grid Radiator

The radiant heat loads were provided by a cylindrical graphite-grid radiator of $4\frac{7}{8}$-inch inside diameter shown in figure 3. The radiator was machined from a solid log of grade 873-S graphite manufactured by the Speer Carbon Company. For both the radiative and combined convective-radiative tests the radiator was placed above the arc jet nozzle as shown in figure 4. The radiator was energized by a single-phase 80-volt alternating-current supply and the current was varied from 1,000 to 2,000 amperes to produce radiative heating rates at the specimen surface from 40 to 200 Btu/ft^2-sec. Oxidation and erosion during the combined convective-radiative tests consumed much of the radiator; hence, each radiator was used for only one or two tests before replacement.

In order to estimate the performance of the cylindrical graphite-grid radiator, calculations based on the radiation configuration factors of references 3 and 4 were made for several radiator temperature levels. These calculations are summarized in the appendix and a comparison of these calculations with the measured performance of the radiator is shown in figure 5.

TEST SPECIMENS

For this preliminary evaluation of the influence of radiative heat loads on ablation materials, two types of ablators were chosen: the subliming ablator and the charring ablator. The subliming ablators used were two forms of molded Teflon - commercial white unfilled Teflon and a filled Teflon, or Fluorogreen, having greater opacity. Both the Teflon and Fluorogreen specimens were used as purchased from commercial fabricators. The charring ablator was a phenolic-nylon molded of equal parts by weight of phenolic powder and nylon powder. The phenolic was BRP-5549 croning resin produced by the Bakelite Corporation, and the nylon was Zytel 103.

L
1
8
2
0

The specimens were machined to disks 3 inches in diameter with thicknesses such that all specimens weighed 0.147 lb or 3 lb/ft^2. For the Teflon specimens this weight gave a thickness of 0.27 inch; for the Fluorogreen specimen, 0.25 inch; and for the less dense phenolic-nylon, 0.48 inch. One surface of the Teflon and Fluorogreen specimens was chemically etched to permit cementing the specimens to the mounting rings.

A copper calorimeter and a guard ring 1/8 inch thick were bonded to the back surface of the specimen. This assembly was then bonded to a brass mounting ring and mounted on a 3-inch-diameter water-cooled sting as shown in figure 6. The design of the water-cooled sting permitted the flange of the mounting ring to be cooled by its contact with the sting so that the back surface of the specimen would not be heated by exposure of its peripheral surface to the heated airstream.

TEST PROCEDURE

For the pure convective tests the arc jet was operated in the configuration shown in figure 1. The performance of the jet was monitored by a 3/8-inch-diameter flat-face heating-rate probe similar to that described in reference 5. The probe used in the present investigation was water cooled to permit continuous operation. When the jet had reached stable operating conditions and the convective heating rate, as measured by the probe, had attained a constant value, the water-cooled sting and specimen assembly were inserted into the jet by a hydraulically actuated rotary inserter. When the specimen back surface experienced a 300° F temperature rise, as measured by a thermocouple in the calorimeter cemented to the specimen, the hydraulic actuator was reversed and the specimen was removed from the jet. On removal of the specimen the heating-rate probe was again inserted to measure the convective heating rate. All the convective tests were made with the specimen surface initially 1 inch above the nozzle exit.

For the combined convective-radiative tests the radiator was mounted coaxially over the arc jet nozzle as shown in figure 4. The radiator was energized first, and when the radiator had attained its equilibrium temperature, the arc jet was started and the foregoing procedure was again followed. The radiator temperature was measured by means of a recording radiometer and occasional collaborating measurements were made with an optical pyrometer. The total heating rate at the specimen location was recorded by the heating-rate probe while the radiator was attaining its equilibrium temperature and while the jet was in operation before the specimen was inserted. After the specimen was removed, the total heating rate was recorded while the jet was in operation, after the jet was terminated, and after the radiator was deenergized. The convective component of the total heating rate was obtained by subtracting the radiative component, measured before and after jet operation, from the total heating rate indicated by the probe. The convective and radiative heating rates for a typical combined convective-radiative heating test are shown in figure 7.

The radiative tests were performed over the arc jet facility as previously described except that the arc was not energized. The jet airflow of 0.35 lb/sec was maintained during the radiative tests to blow the smoke and gases from the specimen surface. For the radiative and combined convective-radiative tests the specimens were initially located 1 inch above the top of the radiator. In a few tests of the phenolic-nylon the temperatures of the specimen surface were measured with the optical pyrometer.

RESULTS AND DISCUSSION

The results of the tests are presented in table II in which the heating rates, temperature histories, and protective efficiencies are summarized.

Specimen Temperature Histories

The temperature histories of the back surfaces of the subliming ablators, Teflon and Fluorogreen, are shown in figure 8(a) and those for the charring ablator, phenolic-nylon, are shown in figure 8(b). The convective and radiative heating rates for each specimen are shown above its temperature-time curve.

From the temperature histories for Teflon (the solid-line curves in fig. 8(a)) it is seen that the back surface attained a temperature rise of 300° F in approximately 50 seconds in the pure convective test

($q_c = 115$, $q_r = 0$). Combining a radiative heat input of 42 Btu/ft^2-sec with a convective input of 82 Btu/ft^2-sec reduced the protection time to 11 seconds, less than one-fourth the protection time under pure convective heating of approximately the same total heating rate. Increasing amounts of radiant heat up to 185 Btu/ft^2-sec reduced the protection time for a 300° F temperature rise to only 3 seconds. The radiant heating test ($q_c = 0$, $q_r = 70$ Btu/ft^2-sec), though having a much lower heating rate than the convective test, had a protection time only one-tenth that of the convective test. This drastic reduction in the protection time caused by the radiative heat input is due primarily to the fact that pure Teflon is transparent to radiant heat.

L
1
8
2
0

Fluorogreen, a modified Teflon product and represented by the dashed-line curves in figure 8(a), behaved very much the same as Teflon in the pure convective test and afforded protection against a 300° F temperature rise for 47 seconds. Additions of radiant heat loads from 50 to 155 Btu/ft^2-sec reduced the protection time to about one-half that for pure convective heating. The radiant heating test, having a heat input equal to that of the convective heating test, offered protection slightly longer than one-half the time for pure convective heating. In the most severe case, however, when the total heating rate was 231 Btu/ft^2-sec, the protection time offered by Fluorogreen was almost seven times that provided by Teflon. This improvement in protection time is due to the silica-base additives in Fluorogreen which increase the opaqueness to thermal radiation.

For the subliming ablators of figure 8(a), the reduction in protection time appears much more dependent on the radiative input q_r than on the total heating rate q_T.

The temperature histories for the charring ablator, phenolic-nylon, are plotted in figure 8(b) to a more compressed time scale. As was true of the subliming ablators, the addition of radiant heat loads to the convective heating effected a reduction in the protection time for a 300° F temperature rise, but this reduction was not as great as that for Fluorogreen nor as drastic as that for Teflon. The reduction in protection time was more dependent on the total heating rate q_T than on the radiative heating rate q_r, in contrast with the sublimers. Accordingly, for phenolic-nylon the time to attain a back-surface temperature rise of 300° F is plotted as a function of the sum of the convective and radiative heating rates in figure 9. It will be noted that all the test points tend to fall on one curve, regardless of the nature of the heat load.

The surface temperatures of the char formed on the phenolic-nylon specimen are shown in figure 10. The test points representing the convective heating tests and those representing the radiative heating tests

fall on two separate straight lines. The temperature measured in one combined convective-radiative heating test falls near the extension of the line determined by the pure convective tests. If this char temperature obtained in the combined heating test were plotted against the radiative component of the total heating rate, it would fall near the line drawn through the radiative-heating test points. It is observed that for heating rates in the range from 60 to 80 Btu/ft^2-sec the radiative heating and convective heating appear to produce approximately the same char surface temperatures for the same heating rates. Above 80 Btu/ft^2-sec the radiative heating produces higher surface temperatures than does the pure convective heating. This lower surface temperature in the convective heating tests is believed to be due to the blocking of the convective heating by mass injection into the boundary layer.

L
1
8
2
0

General Behavior of Materials

The behavior of the three materials in the thermal environment created by the 2,500-kilowatt arc jet and the cylindrical radiator differed with the character of the material. The unfilled Teflon in the pure convective test was completely ablated as the back surface attained a temperature rise of 300° F. As radiant heat was added to the environment, the amount of material ablated was decreased. Under radiative heating only 2 percent of the material was ablated. Obviously, the radiant heat penetrated the unfilled Teflon and heated the back surface to the limiting value, with little heat being absorbed by the material and with little ablation.

Fluorogreen, the filled Teflon, was completely ablated in the pure convective heating environment and also in the radiative and combined convective-radiative environments. The opacity of Fluorogreen permitted ablation to occur in the presence of radiation as well as in the convective environment and thereby lengthened the protection time afforded by this subliming ablator when radiative heating was present.

Phenolic-nylon, the charring ablator, lost 70 to 89 percent of its weight in performing its protective role in the convective, radiative, and combined heating environments. The material remaining, 11 to 30 percent, was all char as determined by visual observation. The weight loss was lower in the radiative tests than in the convective tests because the char erosion was less in the radiative tests. Visual observation revealed no essential differences in the physical structure of the chars obtained from the convective, radiative, and combined heating environments. The grain size of the chars developed at the lower heating rates, whether convective or radiative, was larger than that of the chars developed at the higher heating rates. The density of the char, based on measurements of three well-defined pieces, was 31 lb/ft^3 and did not differ significantly for either radiative or convective heating.

Protective Efficiency

The efficiencies of the three materials as a function of the total cold-wall heating rate are compared in figure 11. The efficiency is defined as the total cold-wall heat input to the specimen, before the back surface experienced a 300° F temperature rise, divided by the initial specimen weight.

For the subliming ablators, Teflon and Fluorogreen, the efficiencies for a convective heat load of 110 Btu/ft^2-sec were about the same; both values were somewhat less than 2,000 Btu/lb. For the charring ablator, phenolic-nylon, at the same convective heating rate the efficiency was 5,600 Btu/lb. For Teflon the addition of a radiative heat load decreased the efficiency by about 75 percent. Increasing amounts of radiant heating, for the range of heating rates used in these tests, produced little or no change in efficiency. Fluorogreen, a Teflon product containing silica-base additives and having less transparency, suffered only a 15-percent decrease in efficiency with the addition of radiant heat input.

I
1
8
2
0

For phenolic-nylon, additions of radiant heat loads, though decreasing the protection time as shown in figure 9, resulted in an increased material efficiency as shown by the upper curve in figure 11. Increasing amounts of either convective or radiant heating resulted in increasing efficiencies. Temperatures on the surface of the char increased from approximately 3,000° F to 4,300° F with increasing heat loads; this indicated that the increased efficiency was due largely to the increased reradiation at the higher temperature.

Comparison of the efficiencies for the convective, radiative, and combined heating conditions for phenolic-nylon reveals the same variation in efficiency as the total heating rate was increased. It may be concluded, then, that for the range of heating rates and the thermal environment of these tests, the efficiency of the charring ablator was not significantly affected by the type of heating.

CONCLUDING REMARKS

The results of a limited experimental evaluation of two types of ablators, subliming and charring, under several combinations of convective and radiative heating, in a heating rate range from 40 to 260 Btu/ft^2-sec and at an enthalpy of 3,000 Btu/lb, indicate the following observations:

The efficiency of a charring ablator at this enthalpy level and over this heating-rate range is not significantly influenced by the

type of heating - that is, convective, radiative, or combined convective and radiative. The efficiency of a charring ablator increases with increasing heating rate due to the increasing surface temperature and the attendant increasing reradiation.

The efficiency of transparent subliming ablators under radiative heating is radically deteriorated because of transmission of radiant energy to the interior and to the back surface. The use of fillers to increase the opacity of the subliming ablator improves the efficiency under radiative heat loads. Under combined convective and radiative heating, the efficiency of a subliming ablator is not appreciably influenced by the magnitude of the total heating rate.

Langley Research Center,
National Aeronautics and Space Administration,
Langley Station, Hampton, Va., March 30, 1962.

APPENDIX

RADIATIVE HEATING RATE PRODUCED BY A CYLINDRICAL RADIATOR ON A FLAT CIRCULAR DISK

The geometric configurations with which this paper is concerned are the hollow circular cylinder and the circular disk shown in figure 12. The hollow circular cylinder represents the graphite-grid radiator and the circular disk represents the irradiated specimen. The circular disk receives radiation from two emitting areas of the radiator: (1) the inside cylindrical surface area A_1 and (2) the annular cross-sectional surface area of the end of the radiator A_2. The radiative heat-transfer rate from these two surfaces to the specimen surface A_3 is calculated in the next two sections.

L
1
8
2
0

The radiative heating rate produced by the high-temperature radiator at the surface of a black-body test specimen is stated in the following equation:

$$q_r = \frac{\sigma\epsilon T^4}{A_3}\left(A_1F_{1,3} + A_2F_{2,3}\right) \tag{1}$$

Cylindrical Emitting Surface

The configuration factor $F_{1,3}$ for the radiative transfer from the inside cylindrical surface A_1 to the specimen surface A_3 is given in reference 3 (eq. (B7)) and is rewritten here as

$$F_{1,3} = \frac{1}{4r_i l_1}\left[\sqrt{l^4 + 2\left(r_i^2 + r_3^2\right)l^2 + \left(r_i^2 - r_3^2\right)^2} - \sqrt{S^4 + 2\left(r_i^2 + r_3^2\right)S^2 + \left(r_i^2 - r_3^2\right)^2} + S^2 - l^2\right] \tag{2}$$

where r_i, r_3, l_1, l, and S are the radii and lengths shown in figure 12.

Annular Emitting Surface

The configuration factor $F_{2,3}$ for the radiative transfer from the annular surface A_2 to the specimen surface A_3 can be obtained from configuration factor algebra by using the equations accompanying configuration A-5 in reference 4 and is given as follows:

$$F_{2,3} = \frac{A_o F_{o,3} - A_i F_{i,3}}{A_o - A_i} \tag{3}$$

L
1
8
2
0

in which

A_o circular area of radius r_o

A_i circular area of radius r_i

$$F_{o,3} = \frac{1}{2}\left(x_o - \sqrt{x_o^2 - 4E^2 D_o^2}\right) \tag{4}$$

$$F_{i,3} = \frac{1}{2}\left(x_i - \sqrt{x_i^2 - 4E^2 D_i^2}\right) \tag{5}$$

where the x, D, and E terms are functions of the radii and lengths as follows:

$$E = r_3/S \tag{6}$$

$$D_o = S/r_o \tag{7}$$

$$D_i = S/r_i \tag{8}$$

$$x_o = 1 + (1 + E^2)D_o^2 \tag{9}$$

$$x_i = 1 + (1 + E^2)D_i^2 \tag{10}$$

Correction for Slots

The hollow circular cylinder used in this investigation was rendered electrically feasible by parallel slots cut alternately from top and

bottom of the cylinder as shown in figure 3. Because the slots do not radiate, the emitting surfaces are the cylindrical and annular areas reduced by the areas of their slots. The slot areas are designated as follows:

A_1' total area of slots in surface area A_1, sq ft

A_2' total area of slots in surface area A_2, sq ft

L
1
8
2
0

Total Heating Rate Produced by Cylindrical Radiator at Surface of Circular Disk Specimen

The total heating rate at the specimen surface is comprised of (1) the fraction $F_{1,3}$ of the heating rate produced by the area $A_1 - A_1'$ and (2) the fraction $F_{2,3}$ of the heating rate produced by the area $A_2 - A_2'$. Thus, equation (1), when corrected for the slots in the radiator, becomes

$$q_r = \frac{\sigma\epsilon T^4}{A_3}\left[F_{1,3}\left(A_1 - A_1'\right) + F_{2,3}\left(A_2 - A_2'\right)\right] \tag{11}$$

Numerical Values

For the cylindrical graphite-grid radiator used in this investigation, the following values apply:

$A_1 = 0.637$ sq ft

$A_1' = 0.066$ sq ft

$A_2 = 0.052$ sq ft

$A_2' = 0.003$ sq ft

$A_3 = 0.049$ sq ft

$F_{2,3} = 0.061$

$F_{1,3} = 0.054$

$l = 0.583$ ft

$l_1 = 0.500$ ft

$r_i = 0.203$ ft

$r_o = 0.240$ ft

$r_3 = 0.125$ ft

$S = 0.083$ ft

$\epsilon = 0.90$

L
1
8
2
0

$\sigma = 4.754 \times 10^{-13}$ Btu/(ft^2)($^\circ$R)^4(sec)

By using equation (11) and these dimensions, the average heating rates have been computed for a range of radiator temperatures from 2,000° F to 5,000° F (2,460° R to 5,460° R). The total radiative heating rate is shown as a function of radiator temperature in figure 5. The results are also presented in table III, in which the radiative contributions of the cylindrical and annular surface areas are shown separately. It is seen that the annular surface contribution is approximately 10 percent of that of the cylindrical surface.

Experimental Verification

In order to evaluate the performance of the cylindrical graphite-grid radiator and to verify the foregoing calculations, the average heating rates produced by the radiator were measured by the 3/8-inch-diameter heating-rate probe described previously in this paper and were also measured by determining the initial rate of temperature rise of five thermocouples mounted on a 1/32-inch-thick by 3-inch-diameter Inconel X disk. The radiator temperature was measured by a recording radiometer. The results of the heating-rate and radiator-temperature measurements are shown as the circled points in figure 5. The experimental performance data confirm the calculated prediction within 15 percent.

REFERENCES

1. Heldenfels, Richard R.: High-Temperature Testing of Aircraft Structures. Rep. 205, AGARD, North Atlantic Treaty Organization (Paris), Oct. 1958.

2. Brooks, William A., Jr., Wadlin, Kenneth L., Swann, Robert T., and Peters, Roger W.: An Evaluation of Thermal Protection for Apollo. NASA TM X-613, 1961.

3. Buschman, Albert J., Jr., and Pittman, Claud M.: Configuration Factors for Exchange of Radiant Energy Between Axisymmetrical Sections of Cylinders, Cones, and Hemispheres and Their Bases. NASA TN D-944, 1961.

4. Hamilton, D. C., and Morgan W. R.: Radiant-Interchange Configuration Factors. NACA TN 2836, 1952.

5. Gardon, Robert: An Instrument for the Direct Measurement of Intense Thermal Radiation. Rev. Sci. Instr., vol. 24, no. 5, May 1953, pp. 366-370.

L
1
8
2
0

L
1
8
2
0

TABLE I.- OPERATING CHARACTERISTICS OF 2,500-KILOWATT ARC JET

[Estimated enthalpy = 3,000 Btu/lb]

Nozzle diameter, in.	Power, kw	Flow rate, lb/sec	Heating rate to 3-inch-diameter flat face, Btu/ft^2-sec
6	1,440	0.11	63
4	1,470	.11	82
4	1,560	.35	110
3	1,860	.35	153

TABLE II.- SUMMARY OF MATERIALS AND TEST CONDITIONS FOR

COMBINED CONVECTIVE-RADIATIVE HEATING TESTS

Test	Material	Density, lb/ft^3	Convective heating rate, Btu/ft^2-sec	Radiative heating rate, Btu/ft^2-sec	Total heating rate, Btu/ft^2-sec	Time to attain 300° F at back surface, sec	Protective efficiency, Btu/lb
1	Teflon	134	115	0	115	49.5	1,900
2			82	42	124	11.0	454
3			72	122	194	4.0	258
4			77	185	262	3.0	262
5			0	70	70	5.5	128
6	Fluorogreen	147	109	0	109	46.5	1,690
7			86	54	140	33.5	1,560
8			80	101	181	25.0	1,510
9			76	155	231	20.5	1,582
10			0	104	104	28.5	987
11	Phenolic-nylon	74.5	63	0	63	240	5,040
12			82	0	82	193	5,250
13			106	0	106	158	5,580
14			153	0	153	128	6,520
15			78	69	147	137	6,710
16			66	119	185	110	6,780
17			80	165	245	102	8,330
18			0	39	39	313	4,070
19			0	76	76	199	5,040
20			0	101	101	166	5,590
21			0	124	124	145	6,000

L
1
8
2
0

TABLE III.- RADIATIVE HEATING RATE PRODUCED

BY CYLINDRICAL RADIATOR

Temperature of radiator, °F	Radiative heating rate produced by $A_1 - A_1'$, Btu/ft^2-sec	Radiative heating rate produced by $A_2 - A_2'$, Btu/ft^2-sec	Total radiative heating rate produced by radiator, Btu/ft^2-sec
Calculated results			
2,460	9.8	0.9	10.7
3,460	38.5	3.7	42.2
3,960	66.1	6.4	72.5
4,460	106.5	10.3	116.8
4,710	132.4	12.8	145.2
4,960	162.9	15.7	178.6
5,210	198.3	19.2	217.5
5,460	239.2	23.1	262.4
Measured results			
2,460			11.1
2,660			14.2
2,913			19.0
3,260			30.1
3,600			44.1
3,860			58.1
4,249			84.6
4,410			97.8
4,857			150.8
5,037			186.0

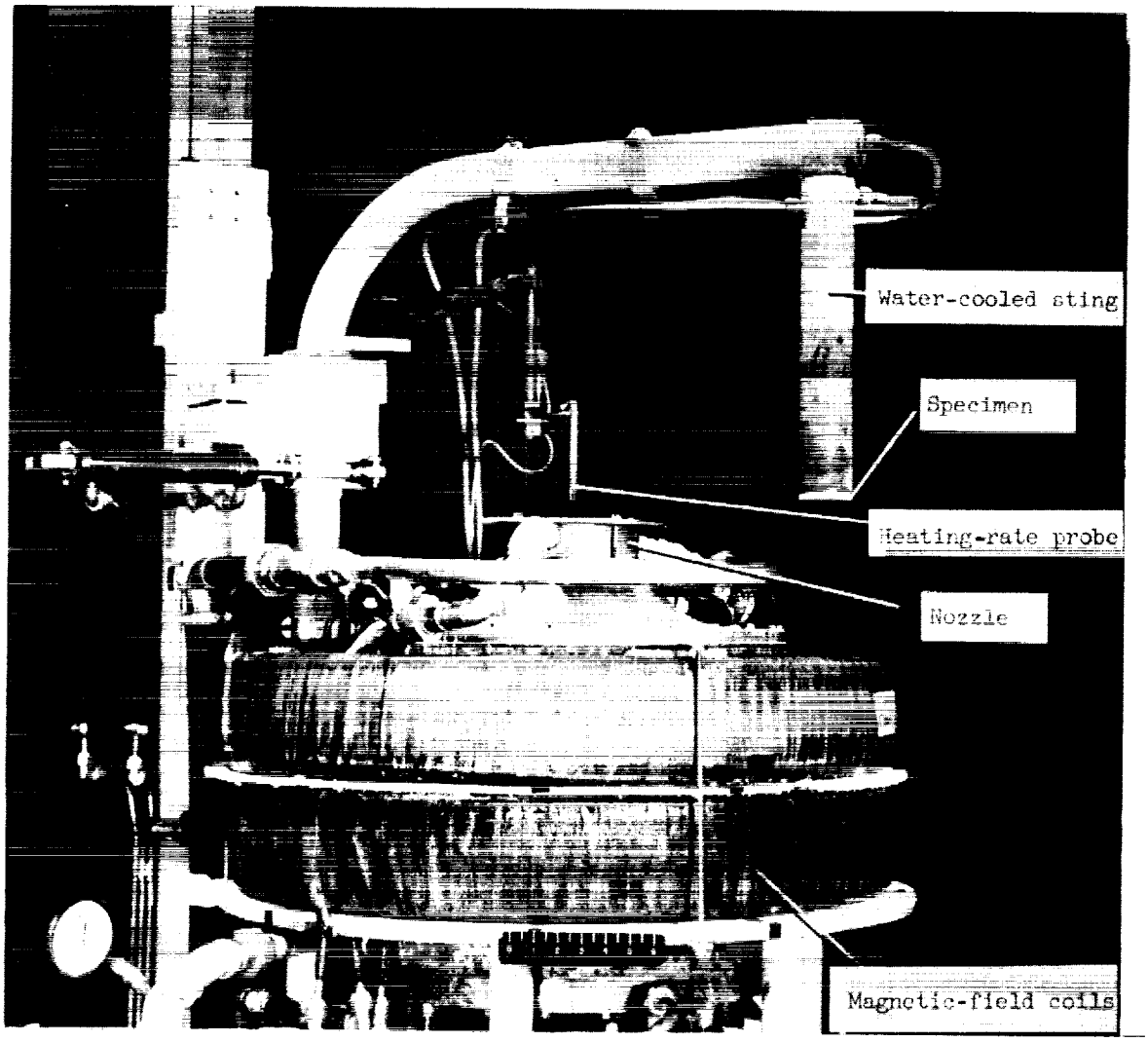

L-1820

L-61-3423.1

Figure 1.- The 2,500-kilowatt arc jet used in convective heating tests.

L-1820

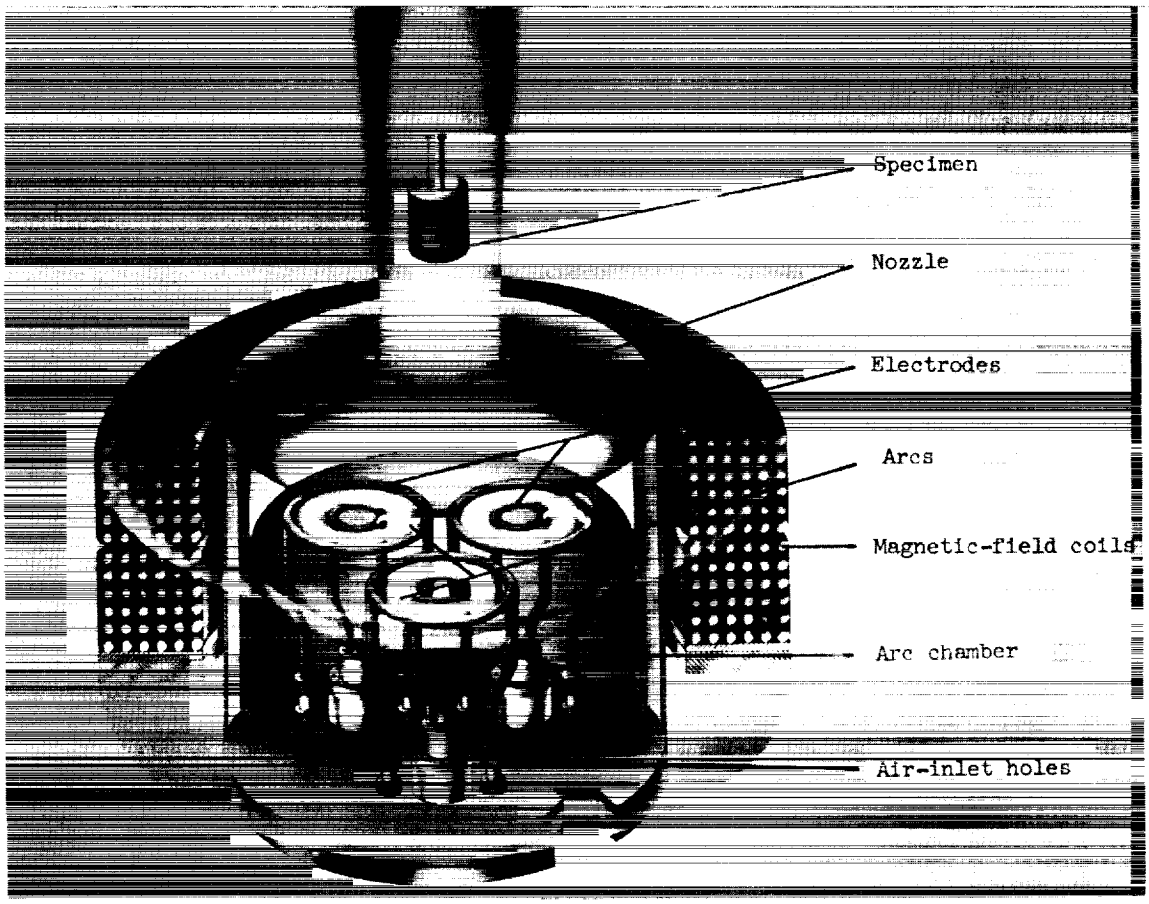

Figure 2.- Phantom view of 2,500-kilowatt arc jet. L-62-99

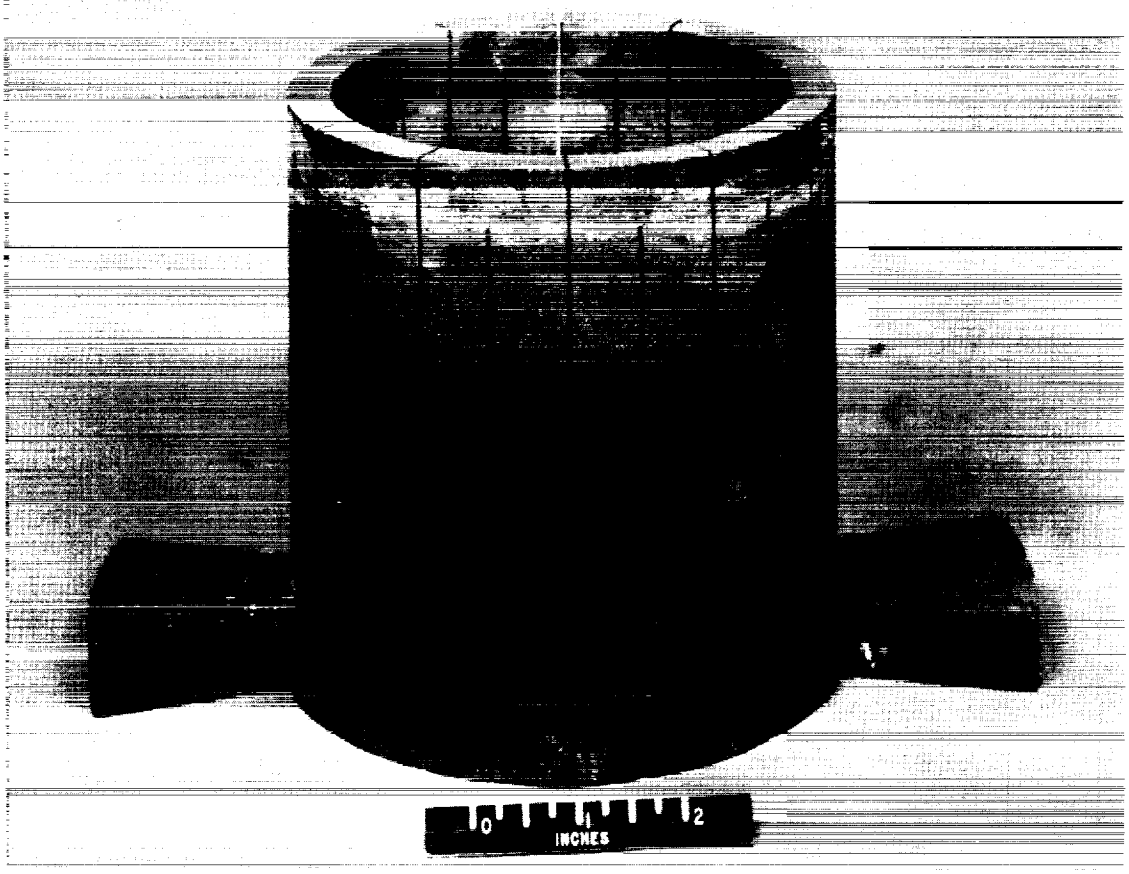

L-1820

L-61-3439

Figure 3.- Cylindrical graphite-grid radiator.

L-1820

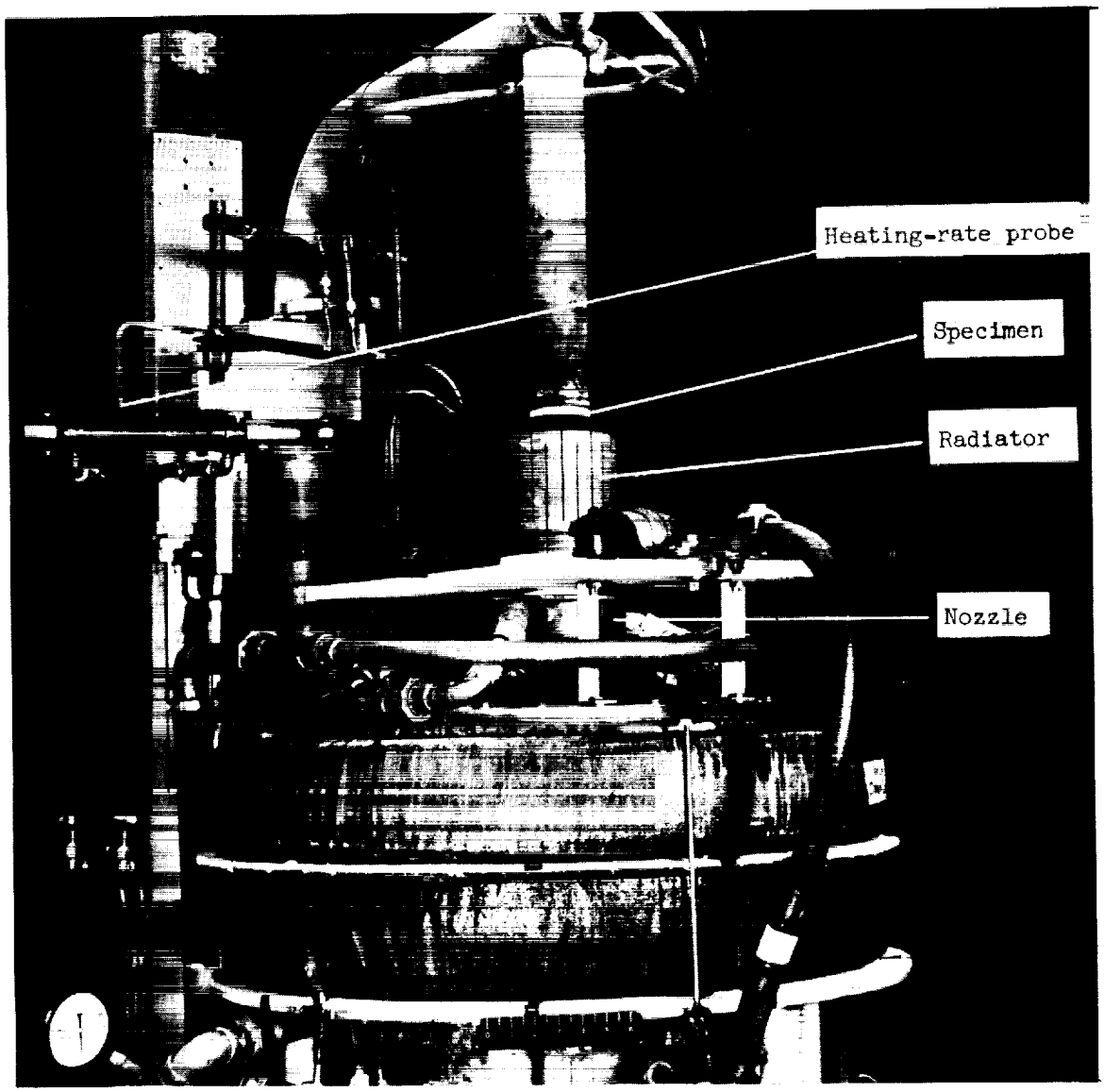

L-61-3421.1

Figure 4.- Radiator mounted on 2,500-kilowatt arc jet.

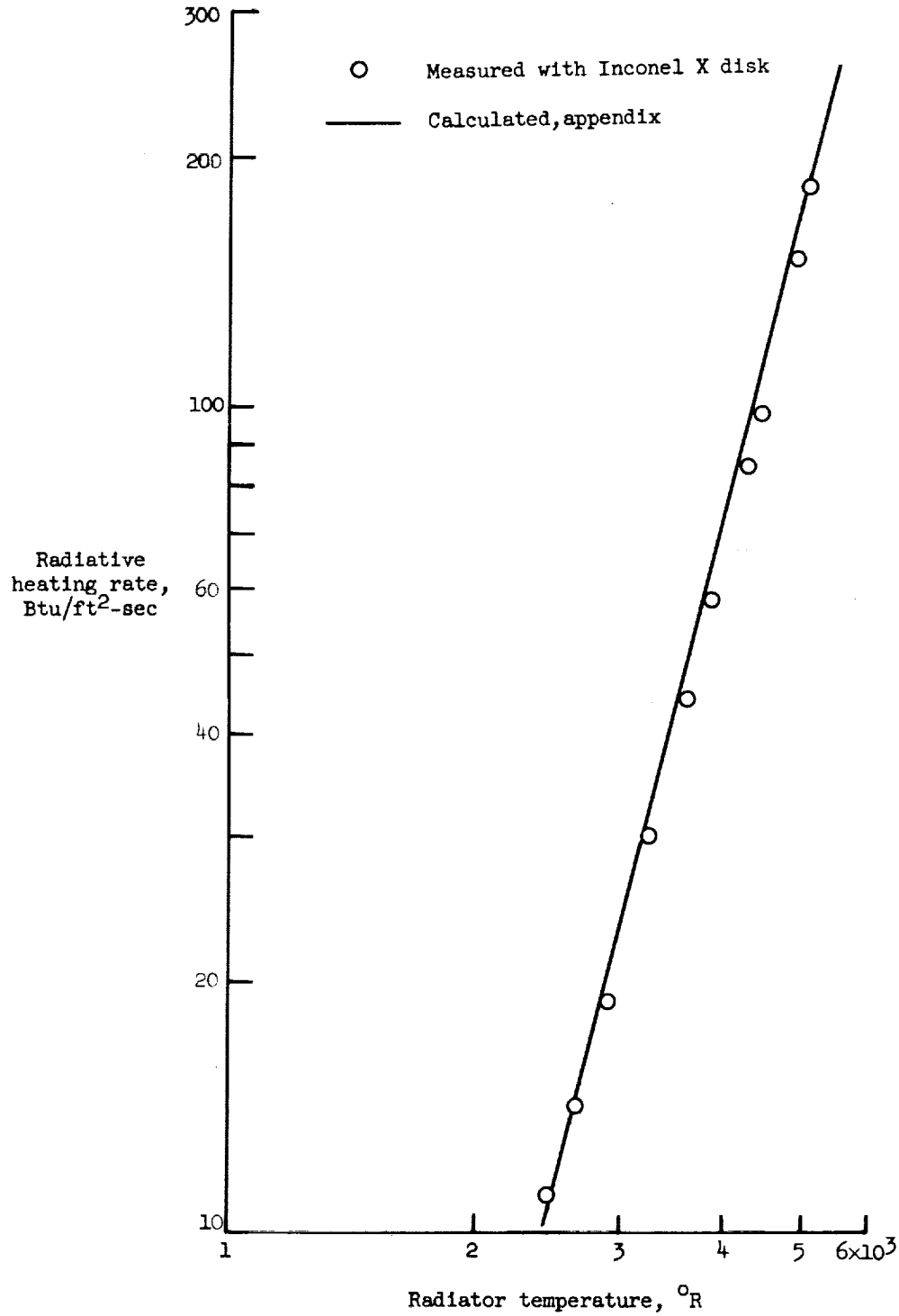

Figure 5.- Radiative heating rate produced by cylindrical radiator.

L-1820

L-1820

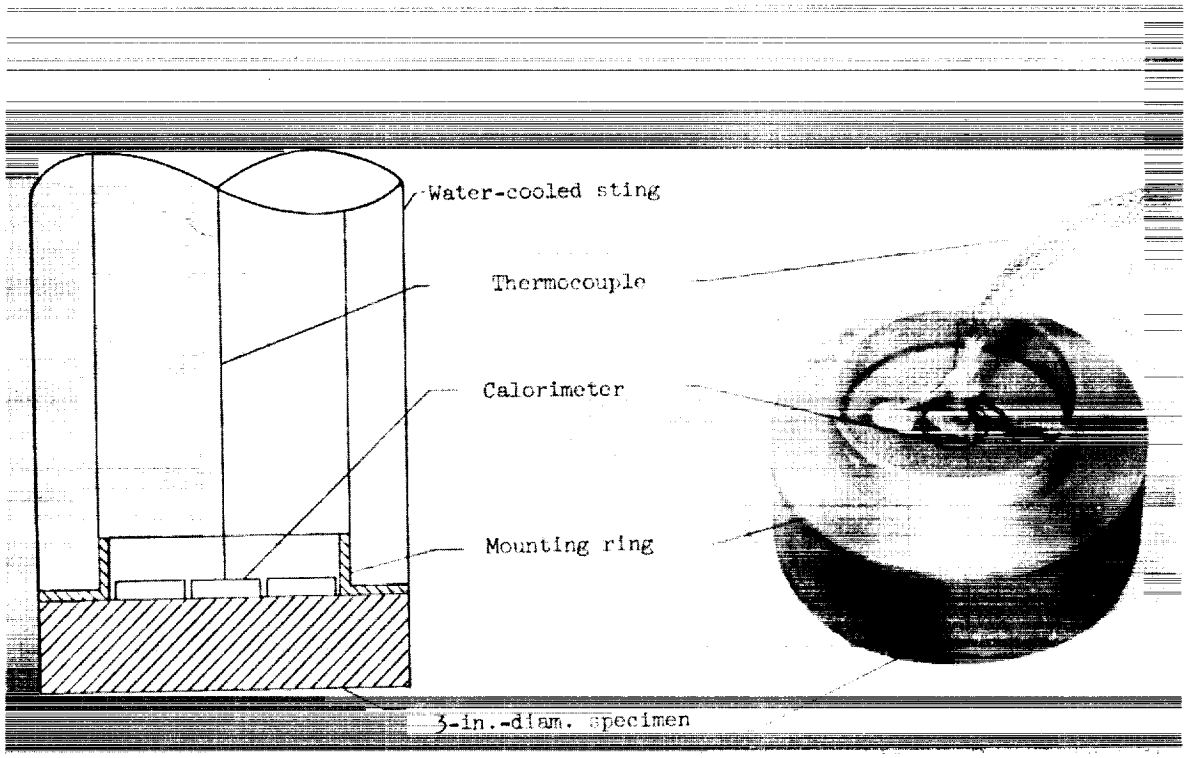

L-62-100

Figure 6.- Details of specimen, mounting, and instrumentation.

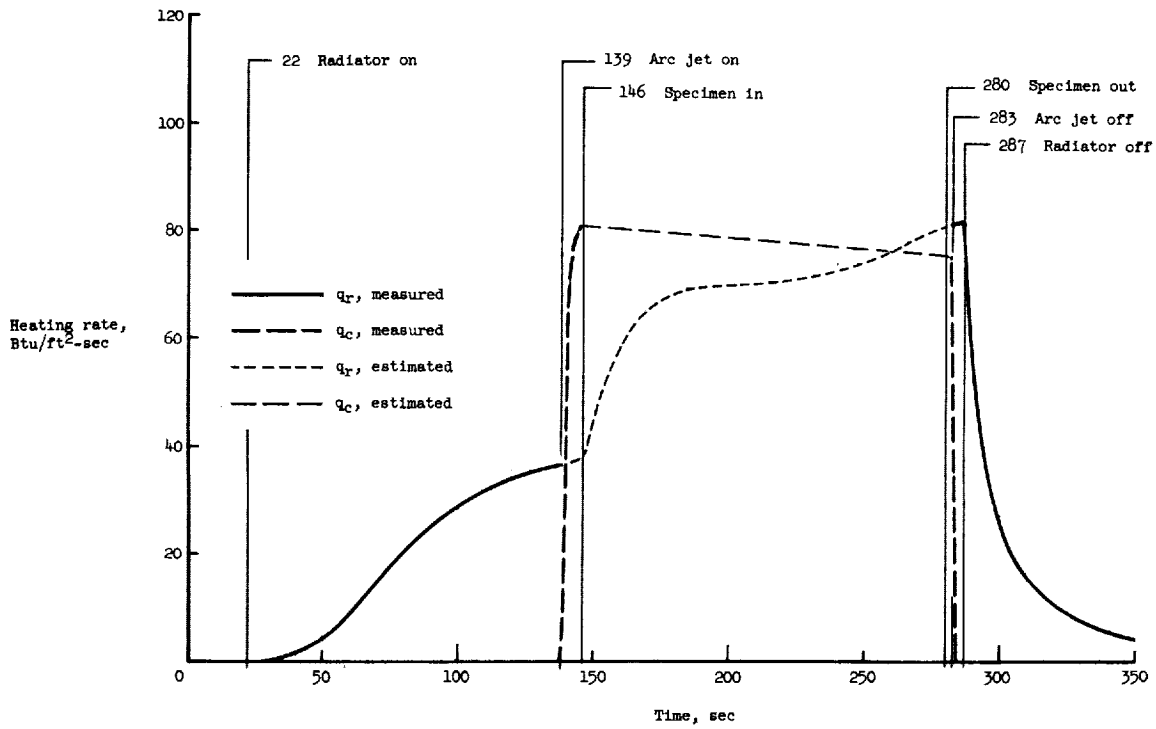

Figure 7.- Convective and radiative heating-rate histories for a typical combined convective-radiative heating test on phenolic-nylon.

L-1820

L-1820

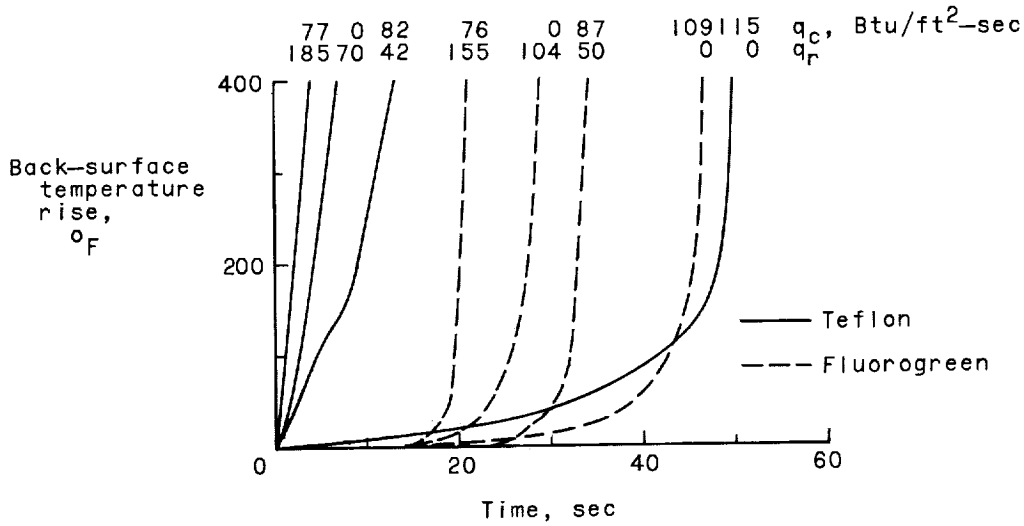

(a) Subliming ablators, Teflon and Fluorogreen.

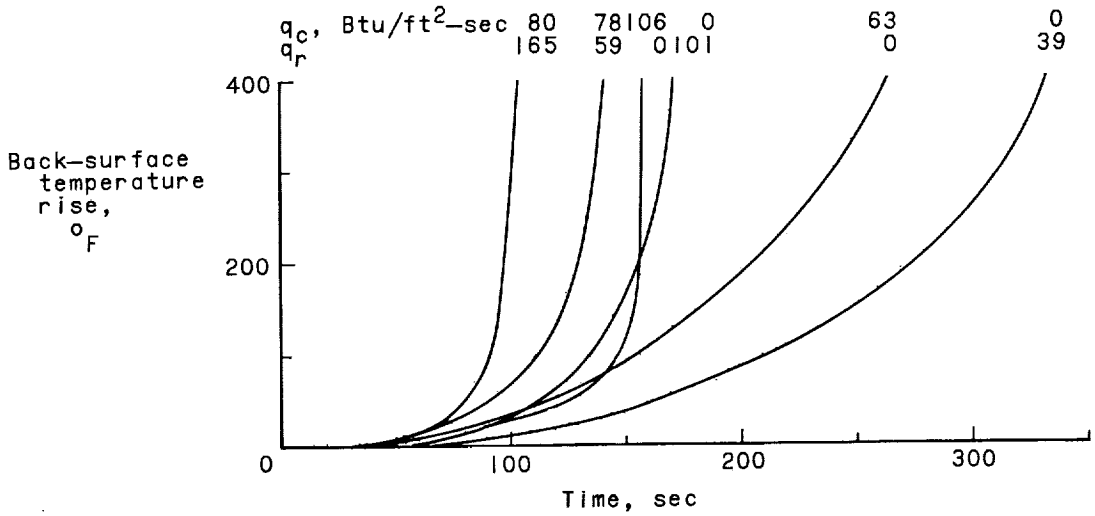

(b) Charring ablator, phenolic nylon.

Figure 8.- Back-surface temperature histories for subliming and charring ablators subjected to convective and radiative heating.

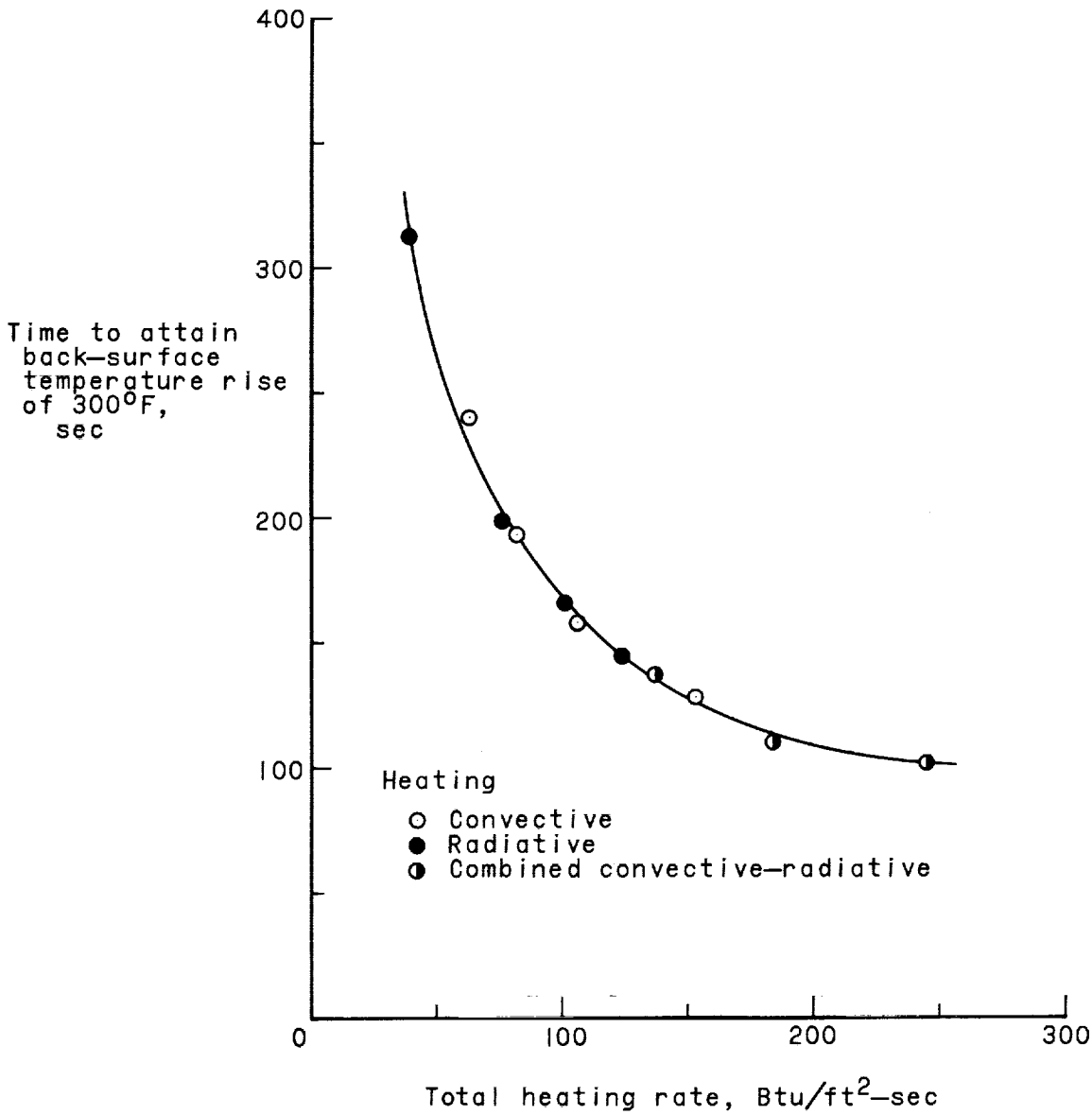

Figure 9.- Effect of heating rate on protection time afforded by phenolic-nylon.

L-1820

L-1820

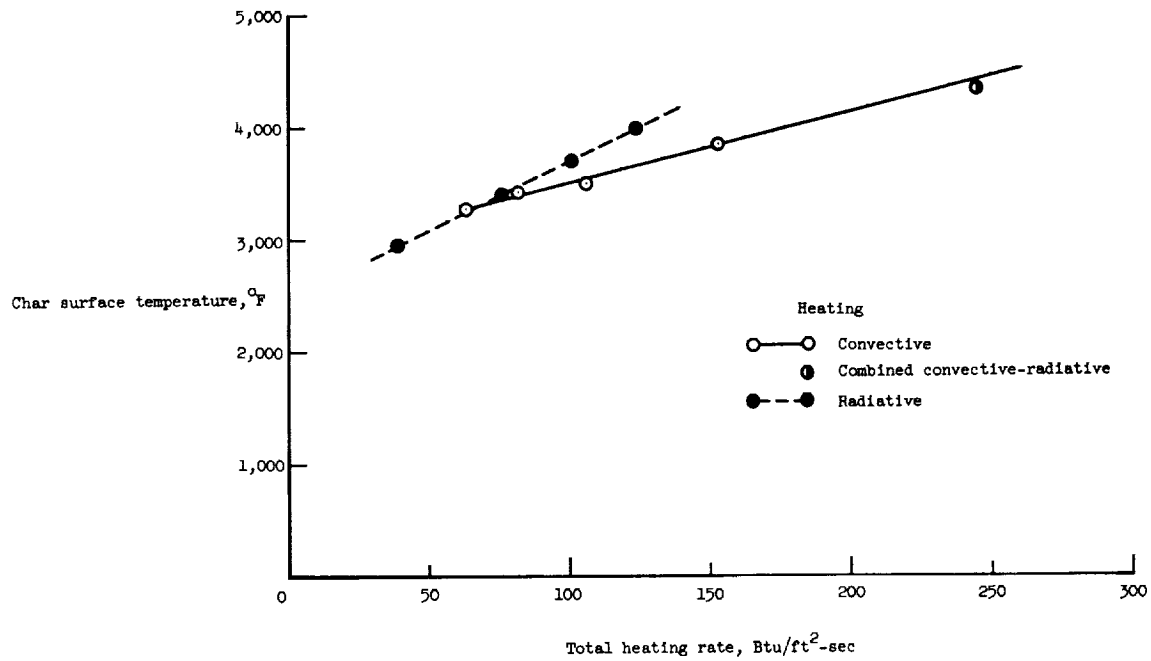

Figure 10.- Effect of total heating rate on the char surface temperature.

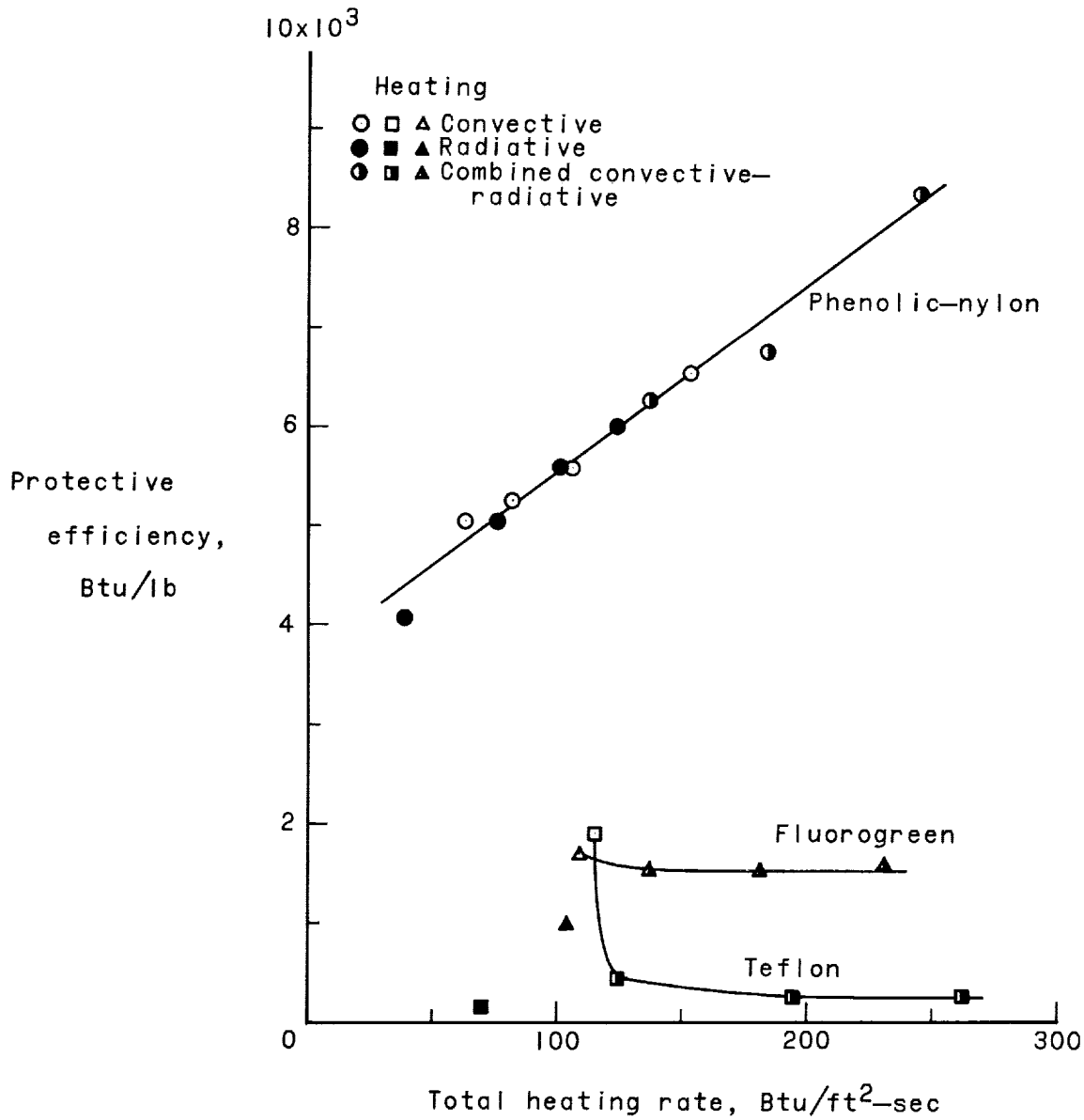

Figure 11.- Effect of radiative heat input on the efficiency of subliming and charring ablators.

L-1820

L-1820

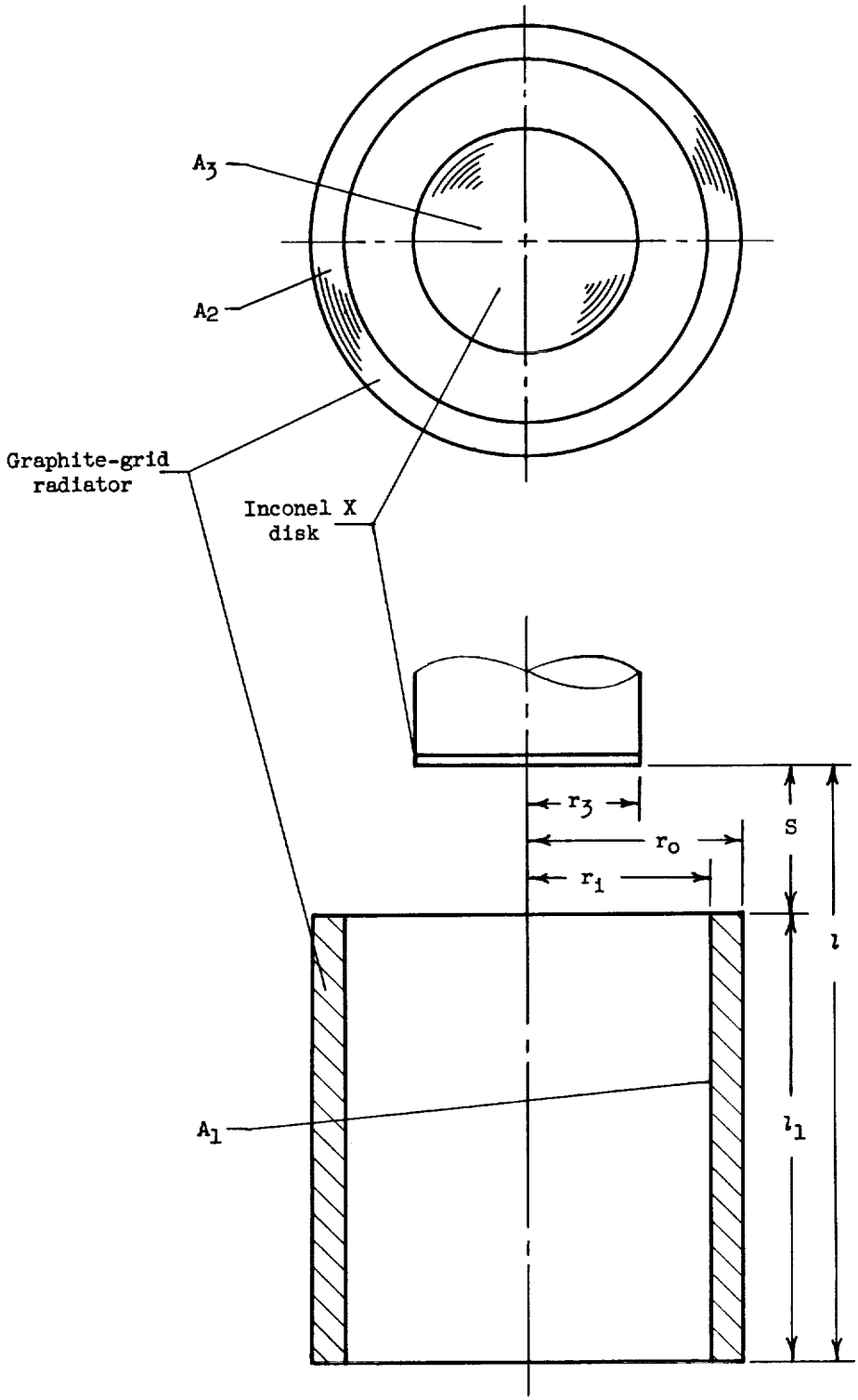

Figure 12.- Configuration for radiant heat transfer from graphite-grid radiator to Inconel X disk.

NASA-Langley, 1962 L-1820

NASA TN D-1355
National Aeronautics and Space Administration.
EXPERIMENTAL INVESTIGATION OF THE EFFECT OF CONVECTIVE AND RADIATIVE HEAT LOADS ON THE PERFORMANCE OF SUBLIMING AND CHARRING ABLATORS. Roger W. Peters and R. Gale Wilson. July 1962. 29p. OTS price, $0.75. (NASA TECHNICAL NOTE D-1355)

A limited number of combined convective heating and radiative heating tests in a subsonic arc jet augmented by a graphite-grid radiator have shown that the efficiency of a subliming ablator, particularly a transparent material, may be greatly reduced by a radiant heat input and that the efficiency of a charring ablator increases with increasing heating rate, regardless of whether the heat input is radiative or convective, because the higher surface temperatures promote increased reradiation.

I. Peters, Roger W.
II. Wilson, R. Gale
III. NASA TN D-1355

(Initial NASA distribution: 2, Aerodynamics, missiles and space vehicles; 5, Atmospheric entry; 20, Fluid mechanics; 26, Materials, other.)

NASA

NASA TN D-1355
National Aeronautics and Space Administration.
EXPERIMENTAL INVESTIGATION OF THE EFFECT OF CONVECTIVE AND RADIATIVE HEAT LOADS ON THE PERFORMANCE OF SUBLIMING AND CHARRING ABLATORS. Roger W. Peters and R. Gale Wilson. July 1962. 29p. OTS price, $0.75. (NASA TECHNICAL NOTE D-1355)

A limited number of combined convective heating and radiative heating tests in a subsonic arc jet augmented by a graphite-grid radiator have shown that the efficiency of a subliming ablator, particularly a transparent material, may be greatly reduced by a radiant heat input and that the efficiency of a charring ablator increases with increasing heating rate, regardless of whether the heat input is radiative or convective, because the higher surface temperatures promote increased reradiation.

I. Peters, Roger W.
II. Wilson, R. Gale
III. NASA TN D-1355

(Initial NASA distribution: 2, Aerodynamics, missiles and space vehicles; 5, Atmospheric entry; 20, Fluid mechanics; 26, Materials, other.)

NASA

NASA TN D-1355
National Aeronautics and Space Administration.
EXPERIMENTAL INVESTIGATION OF THE EFFECT OF CONVECTIVE AND RADIATIVE HEAT LOADS ON THE PERFORMANCE OF SUBLIMING AND CHARRING ABLATORS. Roger W. Peters and R. Gale Wilson. July 1962. 29p. OTS price, $0.75. (NASA TECHNICAL NOTE D-1355)

A limited number of combined convective heating and radiative heating tests in a subsonic arc jet augmented by a graphite-grid radiator have shown that the efficiency of a subliming ablator, particularly a transparent material, may be greatly reduced by a radiant heat input and that the efficiency of a charring ablator increases with increasing heating rate, regardless of whether the heat input is radiative or convective, because the higher surface temperatures promote increased reradiation.

I. Peters, Roger W.
II. Wilson, R. Gale
III. NASA TN D-1355

(Initial NASA distribution: 2, Aerodynamics, missiles and space vehicles; 5, Atmospheric entry; 20, Fluid mechanics; 26, Materials, other.)

NASA

NASA TN D-1355
National Aeronautics and Space Administration.
EXPERIMENTAL INVESTIGATION OF THE EFFECT OF CONVECTIVE AND RADIATIVE HEAT LOADS ON THE PERFORMANCE OF SUBLIMING AND CHARRING ABLATORS. Roger W. Peters and R. Gale Wilson. July 1962. 29p. OTS price, $0.75. (NASA TECHNICAL NOTE D-1355)

A limited number of combined convective heating and radiative heating tests in a subsonic arc jet augmented by a graphite-grid radiator have shown that the efficiency of a subliming ablator, particularly a transparent material, may be greatly reduced by a radiant heat input and that the efficiency of a charring ablator increases with increasing heating rate, regardless of whether the heat input is radiative or convective, because the higher surface temperatures promote increased reradiation.

I. Peters, Roger W.
II. Wilson, R. Gale
III. NASA TN D-1355

(Initial NASA distribution: 2, Aerodynamics, missiles and space vehicles; 5, Atmospheric entry; 20, Fluid mechanics; 26, Materials, other.)

NASA